HS → LS conversion, which depopulates the HS form trapped inthe matrix and converts the complex back into the LS species, which is the thermodynamically stable form at ~80 K. The LIESST conversion at low temperatures and the subsequent "annealing" process at $T > 40$ K are completely reversible, as shown by the fact that successive recycling of the sample through these temperature regimes produced closely replicate results. It may thus be concluded that the LIESST process does not depend on lattice defects produced by sample preparation methods but is, indeed, an intrinsic property of these spin-crossover complexes.

Acknowledgment. This research has been supported by a grant (DMR-8102940) from the Division of Materials Research of the National Science Foundation and the office of the Dean of the Faculty of Arts and Sciences of Rutgers University. The authors are indebted to Dr. J. E. Phillips for the electronic spectra cited in this study and to Profs. J. A. Potenza and H. J. Schugar for a number of illuminating discussions. We are also indebted to Prof. P. Gutlich for generously making available to us a sample of *cis*-$Fe(phen)_2(SCN)_2$ used in his Mössbauer studies for comparison with the present infrared data.

Contribution from the Department of Chemistry, The University of Texas at Austin, Austin, Texas 78712

Synthesis and Structures of Dinuclear Nickel(I) Di-*tert*-butylarsenido Complexes: X-ray Crystal Structures of $[Ni(\mu\text{-}t\text{-}Bu_2As)(PMe_3)]_2$ (Ni–Ni) and $[Ni(\mu\text{-}t\text{-}Bu_2As)(CN\text{-}p\text{-}tol)_2]_2$ (Ni–Ni) (tol = Tolyl)

Richard A. Jones* and Bruce R. Whittlesey

Received August 5, 1985

The reaction of $NiCl_2(PMe_3)_2$ with Li-*t*-Bu_2As in THF at −78 °C gives $[Ni(\mu\text{-}t\text{-}Bu_2As)PMe_3]_2$ (**1**) in 37% yield. **1** reacts with excess *p*-tolyl isocyanide (CN-*p*-tol) in hexane at room temperature to give $[Ni(\mu\text{-}t\text{-}Bu_2As)(CN\text{-}p\text{-}tol)_2]_2$ (**2**) in 47% yield. **1** and **2** are the first dinickel diorganoarsenido complexes to be structurally characterized by X-ray diffraction. Crystal data for **1**: $C_{22}H_{54}As_2Ni_2P_2$, $M_r = 647.89$, monoclinic, $I2/a$ (a nonstandard setting of $C2/c$, No. 15), $a = 16.848$ (3) Å, $b = 12.069$ (1) Å, $c = 17.379$ (3) Å, $\beta = 114.60$ (2)°, $U = 3213.2$ (5) Å^3, $D_{calcd} = 1.339$ g cm^{-3}, $Z = 4$, λ(Mo Kα) = 0.710 69 Å (graphite monochromator), μ(Mo Kα) = 33.24 cm^{-1}, final $R = 0.0399$ ($R_w = 0.0526$) from 2245 observed reflections ($I > 3\sigma(I)$), 2433 measured. Crystal data for **2**: $C_{48}H_{64}As_2Ni_2N_4$, $M_r = 964.34$, monoclinic, $P2_1/n$ (a nonstandard setting of $P2_1/c$, No. 14), $a = 13.320$ (2) Å, $b = 12.889$ (2) Å, $c = 15.042$ (3) Å, $\beta = 111.00$ (2)°, $V = 2410.7$ (5) Å^3, $D_{calcd} = 1.328$ g cm^{-3}, $Z = 2$, λ(Mo Kα) = 0.710 69 Å (graphite monochromator), μ(Mo Kα) = 21.78 cm^{-1}, final $R = 0.0563$ ($R_w = 0.0657$) from 1557 observed reflections ($I > 3\sigma(I)$), 1743 measured. **1** contains two 16-electron Ni(I) atoms bridged by two *t*-Bu_2As groups and linked by a single Ni–Ni bond (Ni–Ni = 2.429 (1) Å). A crystallographically imposed twofold axis passes through each As atom, giving a planar symmetrical central Ni_2As_2 core. Each Ni atom bears a PMe_3 group, which is virtually coplanar with the Ni_2As_2 plane. In **2** the CN-*p*-tol groups give each Ni atom a pseudotetrahedral geometry. The central Ni_2As_2 core is again planar by virtue of a crystallographic center of inversion, which lies at the midpoint of the Ni–Ni bond (Ni–Ni = 2.693 (2) Å). Trends in Ni–Ni bond lengths in these and related complexes are correlated with the electron count on the metal centers and the type of bridging atom.

Introduction

Although there are a number of compounds in which two nickel atoms are linked by dialkylphosphide bridges, there are only two examples of similar complexes containing dialkylarsenide ligands. Neither of these have been characterized crystallographically. The first such compound was $[CpNi(\mu\text{-}AsMe_2)]_2$, which was reported by Hayter[1] in 1963 and which presumably does not contain a nickel–nickel bond. Shortly thereafter, the complex $[NiCl(NO)(\mu\text{-}AsPh_2)]_2$ was synthesized by Kumar and Hieber.[2] Both compounds contain 18-electron nickel atoms in a formal oxidation state of +2. In addition, several heterobimetallic dimethylarsenide-bridged complexes containing nickel have been made, namely, $Cp(CO)_nM(\mu\text{-}AsMe_2)Ni(CO)_3$ ($n = 3$, M = Cr, Mo[3], W;[4] $n = 2$, M = Fe[5]). This paper describes the syntheses and crystal structures of $[Ni(\mu\text{-}As(t\text{-}Bu)_2)(PMe_3)]_2$ (**1**) and $[Ni(\mu\text{-}As(t\text{-}Bu)_2)(CN\text{-}p\text{-}tol)2]_2$ (**2**), which are the first nickel dialkylarsenide complexes to be structurally characterized.

Results and Discussion

$[Ni(\mu\text{-}t\text{-}Bu_2As)(PMe_3)]_2$ (Ni–Ni) (1). The interaction of $NiCl_2(PMe_3)_2$ with 2 equiv of *t*-Bu_2AsLi in THF at −78 °C gives a dark red solution from which black crystals of $[Ni(\mu\text{-}t\text{-}Bu_2As)(PMe_3)]_2$ (**1**) may be isolated in ca. 37% yield. The complex is air-stable for short periods in the solid state but decomposes rapidly in solution when exposed to the air. NMR spectroscopic data (^1H and ^{31}P) is consistent with the solid-state structure as determined by an X-ray diffraction study. The ^1H NMR shows signals at δ 1.43 and 1.39 (relative to Me_4Si, δ 0.0) attributable to the PMe_3 and *t*-Bu groups, respectively. The $^{31}P\{^1H\}$ NMR spectrum shows a singlet δ 20.48 for the PMe_3 ligands. **1** reacts with 2 equiv of I_2 in toluene at room temperature to give *trans*-$Ni(PMe_3)_2I_3$. The crystal structure of this complex has been determined, and it will be described elsewhere.

X-ray Structure of 1. The complex crystallizes in the monoclinic space group $I2/a$ (a nonstandard setting of $C2/c$, No. 15) with half a molecule in the asymmetric unit (four per unit cell). Crystal data and the summary of intensity data collection parameters for **1** are given in Table I. Atomic positional parameters, bond lengths, and bond angles for **1** are presented in Tables II–IV, respectively. A general view of the molecule with the atom-numbering scheme is shown in Figure 1. The structure consists of discrete molecules with no short intermolecular contacts. The As atoms lie on a crystallographically imposed twofold axis, giving the central Ni_2As_2 core a planar geometry. The terminal PMe_3 ligands are arranged so that the Me_3P–Ni–Ni–PMe_3 unit is virtually linear (P–Ni–Ni = P′–Ni′–Ni = 179.37 (3)° giving the molecue a virtually D_{2h} symmetry. The Ni–Ni distance of 2.429 (1) Å is in accord with a single metal–metal bond, giving each Ni atom an unsaturated 16-electron configuration. This distance is somewhat larger than that found in the *t*-Bu_2P analogue of **1** (2.375 (3) Å), which we recently described.[6] The reason for this

(1) $(CpNiAsMe_2)_2$: Hayter, R. G. *Inorg. Chem.* **1962**, *2*, 1031.
(2) $(NiCl(NO)AsPh_2)_2$: Hieber, W.; Kummer, R. *Z. Anorg. Allg. Chem.* **1966**, *344*, 292.
(3) Madach, T.; Vahrenkamp, H. *Z. Naturforsch., B: Anorg. Chem., Org. Chem.* **1979**, *34*, 1195.
(4) Panster, P.; Malisch, W. *Chem. Ber.* **1976**, *109*, 3842.
(5) Müller, R.; Vahrenkamp, H. *Chem. Ber.* **1977**, *110*, 3910.
(6) Jones, R. A.; Stuart, A. L.; Atwood, J. L.; Hunter, W. E.; Rogers, R. D. *Organometallics* **1982**, *1*, 1721. Jones, R. A.; Stuart, A. L.; Atwood, J. L.; Hunter, W. E. *Organometallics* **1983**, *2*, 874.

0020-1669/86/1325-0852$01.50/0

Table I. Crystal Data and Summary of Intensity Data Collection and Structure Refinement for **1** and **2**

	$C_{22}H_{54}As_2Ni_2P_2$ (**1**)	$C_{48}H_{64}As_2Ni_2N_4$ (**2**)
mol wt	647.89	964.34
space group	$I2/a$ (nonstd setting of $C2/c$, No. 15)	$P2_1/n$ (nonstd setting of $P2_1/c$, No. 14)
cell constants		
a, Å	16.848 (3)	13.320 (2)
b, Å	12.069 (1)	12.889 (2)
c, Å	17.379 (3)	15.042 (3)
β, deg	114.60 (2)	111.00 (2)
cell vol, Å^3	3213.2 (5)	2410.7 (5)
molecules/unit cell	4	2
D(calcd), g cm^{-3}	1.339	1.328
μ(calcd), cm^{-1}	33.24	21.78
radiation, Å	Mo Kα, 0.710 69	Mo Kα, 0.710 69
max cryst dimens, mm	0.20 × 0.20 × 0.20	0.10 × 0.25 × 0.25
scan width, deg	0.8 + 0.35 tan θ	0.8 + 0.35 tan θ
std reflecns	10,0,$\bar{1}$0, $\bar{8}$,0,10	118, 80$\bar{4}$
decay of stds	<0.3%	<0.5%
reflecns measd	2433	1743
2θ range, deg	2–60	2–50
reflcns obsd ($I > 3\sigma(I)$)	2245	1557
no. of parameters varied	128	163
data/parameter ratio	17.537	9.552
R	0.0399	0.0563
R_w	0.0526	0.0657

Table II. Positional Parameters and Their Estimated Standard Deviations for **1**

atom	x	y	z	B,[a] Å^2
As1	0.250	0.38841 (7)	0.500	3.48 (2)
As2	0.250	0.07162 (7)	0.500	3.27 (2)
Ni	0.18244 (4)	0.22939 (6)	0.43616 (4)	3.26 (2)
P	0.0643 (1)	0.2275 (2)	0.3247 (1)	4.50 (4)
C1	0.0154 (6)	0.0947 (7)	0.2771 (6)	10.5 (3)
C2	0.0669 (6)	0.2935 (8)	0.2317 (5)	8.9 (3)
C3	−0.0300 (5)	0.296 (1)	0.3310 (6)	10.8 (3)
C10	0.3086 (4)	0.4832 (5)	0.4441 (4)	5.0 (2)
C11	0.3523 (5)	0.3965 (7)	0.4078 (9)	9.2 (2)
C12	0.2411 (5)	0.5540 (7)	0.3712 (5)	8.1 (3)
C13	0.3802 (5)	0.5576 (7)	0.5093 (5)	8.1 (2)
C20	0.3068 (4)	−0.0240 (6)	0.4412 (4)	5.3 (2)
C21	0.3445 (5)	0.0621 (7)	0.3997 (5)	11.2 (3)
C22	0.3815 (5)	−0.0928 (7)	0.5056 (5)	8.5 (3)
C23	0.2403 (5)	−0.0995 (7)	0.3734 (5)	9.2 (3)

[a] Anisotropically refined atoms are given in the form of the isotropic equivalent thermal parameter defined as $^4/_3[a^2B_{11} + b^2B_{22} + c^2B_{33} + ab(\cos\gamma)B_{12} + ac(\cos\beta)B_{13} + bc(\cos\alpha)B_{23}]$.

Table III. Bond Distances (Å) for **1**[a]

atom 1	atom 2	dist	atom 1	atom 2	dist
As1	Ni	2.271 (1)	P	C3	1.832 (5)
As1	C10	2.006 (4)	C10	C11	1.557 (6)
As2	Ni	2.259 (1)	C10	C12	1.559 (6)
As2	C20	2.027 (4)	C10	C13	1.551 (6)
Ni	Ni′	2.429 (1)	C20	C21	1.544 (7)
Ni	P	2.123 (1)	C20	C22	1.533 (6)
P	C1	1.834 (5)	C20	C23	1.542 (6)
P	C2	1.819 (5)			

[a] Numbers in parentheses are estimated standard deviations in the least significant digits. Primed atoms in **1** are related to the unique atoms by a crystallographic twofold rotation axis.

difference is no doubt due to the larger covalent radius of As in the bridging positions. (Covalent radii: As, 1.22 Å; P, 1.10 Å).[7] There are a few phosphido-bridged analogues of **1** that have also been reported.[8] The di-*tert*-butylarsenido bridge is fairly symmetrical (Ni–As(1) = 2.271 (1) Å, Ni–As(2) = 2.259 (1) Å) while the Ni–P distance of 2.123 (1) Å can be compared to a similar length of 2.136 (5) Å in $[Ni(\mu\text{-}t\text{-}Bu_2P)(PMe_3)]_2$.[6]

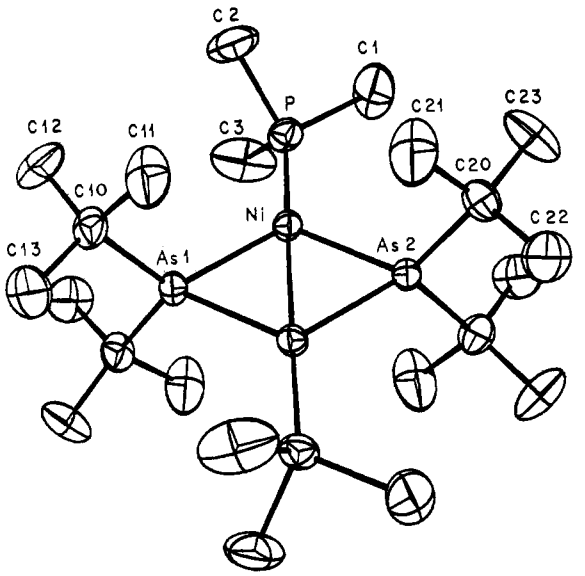

Figure 1. ORTEP view of **1**, showing 30% probability thermal ellipsoids.

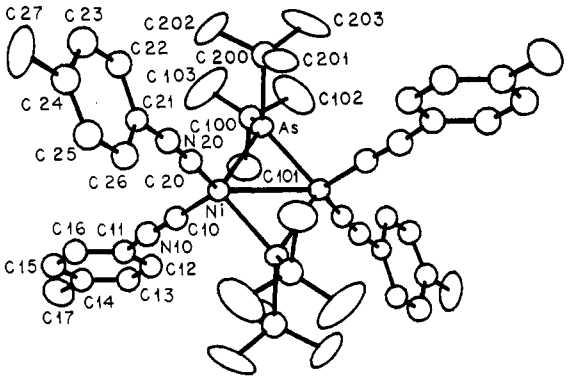

Figure 2. ORTEP view of **2**, showing 30% probability thermal ellipsoids.

[Ni(μ-*t*-Bu$_2$As)(*p*-tol-NC)$_2$]$_2$ (Ni–Ni) (2). The reaction of **1** with excess *p*-tolyl isocyanide in hexane at room temperature results in loss of PMe_3 and the formation of $[Ni(\mu\text{-}t\text{-}Bu_2As)(p\text{-tol-NC})_2]_2$ (**2**) in reasonable yield (47%). The complex is very dark red-black and is moderately air-stable in the solid state. ^{1}H NMR data are in accord with the X-ray crystal structure (see Experimental Section).

X-ray Structure of 2. The complex crystallizes in the monoclinic space group $P2_1/n$ with half a molecule in the asymmetric unit (two per unit cell). A view of the molecule is shown in Figure 2. Details of data collection, crystal data, and refinement are given in Table I. Positional parameters, bond lengths, and angles are presented in Tables V–VII, respectively.

The central Ni_2As_2 core is again planar with a crystallographically imposed center of inversion at the midpoint of the Ni–Ni bond. Two isocyanide ligands replace one PMe_3 group on each Ni. This is reasonable since the steric demand of a *p*-tol-NC group is probably less than that of PMe_3. The coordination geometry about each Ni atom is now pseudotetrahedral,

(7) *Spec. Publ.—Chem. Soc.* **1958**, *No. 11*; **1965**, *No. 18*.

(8) Deppish, B.; Schäfer, H. *Z. Anorg. Allg. Chem.* **1982**, *490*, 129. $[Ni(\mu\text{-}Cy_2P)(Cy_2PH)]_2$ has been described although the X-ray structure has not been reported. Nobile, C. F.; Vasapollo, G.; Giannoccaro, P.; Sacco, A. *Inorg. Chim. Acta* **1981**, *48*, 261. Ni–Ni distances range from ca. 2.33 to 2.80 Å. See also: Mills, O. S.; Shaw, B. W. *J. Organomet. Chem.* **1968**, *11*, 595. Wilkinson, G.; Stone, F. G. A., Abel, E. W., Eds. "Comprehensive Organometallic Chemistry"; Pergamon Press: Elmsford, NY, 1982; Vol. 9, p 1388, and references therein.

Table IV. Bond Angles (deg) for **1**[a]

atom 1	atom 2	atom 3	angle	atom 1	atom 2	atom 3	angle
Ni	As1	Ni′	64.65 (3)	C1	P	C2	98.9 (3)
Ni	As1	C10	119.5 (1)	C1	P	C3	100.5 (3)
Ni	As1	C10′	118.1 (1)	C2	P	C3	101.4 (3)
C10	As1	C10′	110.4 (3)	As1	C10	C11	102.9 (3)
Ni	As2	Ni′	65.06 (3)	As1	C10	C12	111.5 (3)
Ni	As2	C20	118.7 (1)	As1	C10	C13	111.5 (3)
C20	As2	C20′	110.6 (3)	C11	C10	C12	110.3 (5)
As1	Ni	As2	115.14 (2)	C11	C10	C13	109.3 (4)
As1	Ni	Ni′	57.67 (1)	C12	C10	C13	111.1 (4)
As1	Ni	P	122.95 (4)	As2	C20	C21	103.0 (3)
As2	Ni	Ni′	57.47 (1)	As2	C20	C22	110.9 (3)
As2	Ni	P	121.91 (4)	As2	C20	C23	112.1 (3)
Ni′	Ni	P	179.37 (3)	C21	C20	C22	109.5 (5)
Ni	P	C1	119.7 (2)	C21	C20	C23	110.5 (5)
Ni	P	C2	116.4 (2)	C22	C20	C23	110.6 (5)
Ni	P	C3	116.6 (2)				

[a] Numbers in parentheses are estimated standard deviations in the least significant digits. Primed atoms in **1** are related to the unique atoms by a crystallographic twofold rotation axis.

Table V. Positional Parameters and Their Estimated Standard Deviations for **2**

atom	*x*	*y*	*z*	*B*, Å^2
As	0.8537 (1)	0.0356 (1)	0.94664 (9)	3.75 (3)
Ni	1.0193 (1)	0.0868 (2)	1.0533 (1)	3.59 (4)
N10	1.0779 (9)	0.287 (1)	0.9869 (8)	5.3 (3)*
N20	1.0007 (8)	0.096 (1)	1.2444 (7)	4.6 (3)*
C10	1.056 (1)	0.206 (1)	1.0112 (9)	4.6 (3)*
C11	1.095 (1)	0.372 (1)	0.9361 (9)	4.8 (3)*
C12	1.094 (1)	0.358 (1)	0.844 (1)	4.9 (3)*
C13	1.104 (1)	0.445 (1)	0.792 (1)	5.5 (4)*
C14	1.118 (1)	0.541 (1)	0.8305 (9)	5.2 (3)*
C15	1.118 (1)	0.555 (1)	0.922 (1)	5.6 (4)*
C16	1.108 (1)	0.468 (1)	0.976 (1)	5.5 (3)*
C17	1.126 (1)	0.637 (1)	0.773 (1)	7.7 (5)
C20	1.009 (1)	0.088 (1)	1.1686 (9)	4.2 (3)*
C21	0.9998 (9)	0.110 (1)	1.3364 (8)	3.7 (3)*
C22	0.904 (1)	0.138 (1)	0.3469 (9)	4.8 (3)*
C23	0.908 (1)	0.156 (1)	1.442 (1)	6.3 (4)*
C24	1.006 (1)	0.148 (1)	1.518 (1)	5.6 (4)*
C25	1.096 (1)	0.114 (1)	1.506 (1)	5.7 (4)*
C26	1.095 (1)	0.096 (1)	1.4124 (9)	5.1 (3)*
C27	1.005 (2)	0.171 (2)	1.621 (1)	9.4 (6)
C100	0.781 (1)	0.118 (1)	0.824 (1)	5.2 (4)*
C101	0.869 (1)	0.153 (1)	0.789 (1)	7.2 (5)
C102	0.705 (2)	0.049 (2)	0.749 (1)	12.4 (8)
C103	0.725 (2)	0.213 (2)	0.843 (1)	13.5 (7)
C200	0.737 (1)	0.001 (1)	1.001 (1)	5.6 (4)*
C201	0.790 (1)	−0.072 (1)	1.086 (1)	6.7 (4)
C202	0.699 (1)	0.099 (2)	1.037 (1)	10.5 (5)
C203	0.646 (1)	−0.061 (2)	0.928 (1)	12.1 (7)

[a] Starred atoms were refined isotropically. Anisotropically refined atoms are given in the form of the isotropic equivalent thermal parameter defined as in Table II.

Table VI. Bond Distances (Å) for **2**

atom 1	atom 2	dist	atom 1	atom 2	dist
As	Ni	2.310 (1)	C14	C17	1.537 (12)
As	Ni′	2.312 (1)	C15	C16	1.419 (11)
As	C100	2.047 (9)	C21	C22	1.389 (10)
As	C200	2.042 (9)	C21	C26	1.382 (10)
Ni	Ni′	2.693 (2)	C22	C23	1.434 (11)
Ni	C10	1.789 (9)	C23	C24	1.401 (11)
Ni	C20	1.789 (8)	C24	C25	1.352 (11)
N10	C10	1.180 (9)	C24	C27	1.584 (12)
N10	C11	1.403 (10)	C25	C26	1.424 (11)
N20	C20	1.189 (8)	C100	C101	1.519 (12)
N20	C21	1.399 (9)	C100	C102	1.509 (13)
C11	C12	1.392 (11)	C100	C103	1.500 (14)
C11	C16	1.355 (11)	C200	C201	1.541 (12)
C12	C13	1.398 (11)	C200	C202	1.530 (13)
C13	C14	1.355 (11)	C200	C203	1.540 (13)
C14	C15	1.392 (11)			

[a] Numbers in parentheses are estimated standard deviations in the least significant digits. Primed atoms in **2** are related to the unique atoms by a crystallographic inversion center.

and each metal achieves an 18-electron count via a single Ni–Ni bond. The 18- vs 16-electron count on the metal has a dramatic effect on the Ni–Ni distance, which is now 2.693 (2) Å. Table VIII shows how the formally single Ni–Ni bond varies in these and related complexes. The Ni–Ni single-bond lengths fall within values that have previously been reported for such distances.[6] The trends in Ni–Ni distances may be rationalized in terms of variations in electron count of the metal, the type of bridging atom, and the nature of L. Thus the 16e–16e phosphide-bridged complexes $[Ni(\mu\text{-}t\text{-}Bu_2P)(PMe_3)]_2$,[6] $[Ni(\mu\text{-}(Me_3Si)_2P)(PMe_3)]_2$,[8] and $[Ni(\mu\text{-}P(cy)_2)(C_2H_4)]_2$[9] have the shortest Ni–Ni bonds of 2.375 (3), 2.381 (1), and 2.388 (1) Å, respectively. The asymmetric compounds $(CO)_2Ni(\mu\text{-}t\text{-}Bu_2P)_2Ni(PMe_3)$ and $(CO)_2Ni(\mu\text{-}t\text{-}Bu_2P)_2Ni(CO)$ of structure type B have slightly longer Ni–Ni distances (2.446 (2) and 2.414 (2) Å). The metals in these complexes have formally 16- and 18-electron counts. The 18e–18e systems such as $[Ni(\mu\text{-}PPh_2)(CO)_2]_2$[10] and $[Ni(\mu\text{-}t\text{-}BuHP)(PMe_3)_2]_2$[11] have even longer Ni–Ni distances of 2.51 and 2.559 (2) Å, respectively. This increase in bond length no doubt reflects the increasing electron density on the metals. Thus a Ni–Ni bond between two 16-electron Ni atoms is notably shorter than that between two 18-electron nickels. On replacement of the bridging P atoms with As, the Ni(16e)–Ni(16e) distance increases from 2.375 (3) to 2.429 (1) Å in **1** as expected. The Ni(18e)–Ni(18e) complex **2** then has the longest Ni–Ni bond of these compounds (2.693 (2) Å), again consistent with increased electron density on the metals. The Ni–As distances of 2.310 (1) and 2.312 (1) Å are both slightly longer than those observed in **1** (2.265 Å (av)), which is a consequence of the longer Ni–Ni bond. The coordination geometry about each Ni is distorted from a perfect tetrahedron. Thus As–Ni–As = 108.74 (5)° while C(20)–Ni–C(10) = 117.5 (4)° and C(20)–Ni–As = 106.8 (3)°. Such distortions are not unexpected in view of the different groups attached to Ni. The other structural parameters of the molecule are normal.

Experimental Section

All reactions were performed under oxygen-free nitrogen or under vacuum. Hexane, THF, and diethyl ether were dried over sodium and distilled form sodium/benzophenone under nitrogen before use. Melting points were in sealed capillaries under nitrogen (1 atm) and are uncor-

(9) Barnett, B. L.; Kruger, C. *Cryst. Struct. Commun.* **1973**, *2*, 85.

(10) Jarvis, J. A.; Mais, R. H. B.; Owston, P. G.; Thompson, D. T. *J. Chem. Soc. A* **1970**, 1867.

(11) Jones, R. A.; Norman, N. C.; Seeberger, M. H.; Atwood, J. L.; Hunter, W. E. *Organometallics* **1983**, *2*, 1629.

Table VII. Bond Angles (deg) for **2**[a]

atom 1	atom 2	atom 3	angle	atom 1	atom 2	atom 3	angle
Ni	As	Ni′	71.26 (5)	C15	C14	C17	118.6 (9)
Ni	As	C100	120.2 (3)	C14	C15	C16	119.3 (9)
Ni	As	C200	117.2 (3)	C11	C16	C15	120.0 (8)
Ni′	As	C100	117.8 (3)	Ni	C20	N20	175.4 (8)
Ni′	As	C200	120.8 (3)	N20	C21	C22	118.6 (7)
C100	As	C200	106.7 (4)	N20	C21	C26	118.1 (7)
As	Ni	As′	108.74 (5)	C22	C21	C26	123.3 (8)
As	Ni	Ni′	54.41 (4)	C21	C22	C23	116.7 (8)
As	Ni	C10	108.1 (3)	C22	C23	C24	119.8 (9)
As	Ni	C20	106.8 (3)	C23	C24	C25	121.8 (9)
As′	Ni	Ni′	54.33 (4)	C23	C24	C27	116.9 (9)
As′	Ni	C10	107.1 (3)	C25	C24	C27	121.2 (9)
As′	Ni	C20	108.5 (3)	C24	C25	C26	119.5 (8)
Ni′	Ni	C10	121.2 (3)	C21	C26	C25	118.7 (8)
Ni′	Ni	C20	121.3 (3)	As	C100	C101	106.9 (6)
C10	Ni	C20	117.5 (4)	As	C100	C102	110.0((7)
C10	N10	C11	166.1 (9)	As	C100	C103	111.3 (7)
C20	N20	C21	175.0 (8)	C101	C100	C102	107.9 (9)
Ni	C10	N10	176.5 (8)	C101	C100	C103	109.0 (1)
N10	C11	C12	120.0 (8)	C102	C100	C103	112.0 (1)
N10	C11	C16	119.5 (8)	As	C200	C201	105.9 (6)
C12	C11	C16	120.4 (9)	As	C20	C202	111.5 (7)
C11	C12	C13	119.5 (9)	As	C200	C203	110.4 (7)
C12	C13	C14	120.8 (8)	C201	C200	C202	108.6 (8)
C13	C14	C15	120.0 (9)	C201	C200	C203	106.4 (9)
C13	C14	C17	121.2 (8)	C202	C200	C203	114.1 (1)

[a] Numbers in parentheses are estimated standard deviations in the least significant digits. Primed atoms in **2** are related to the unique atoms by a crystallographic inversion center.

Table VIII. Comparison of Ni–Ni Distances in a Series of Phosphido- and Arsenido-Bridged Dinuclear Complexes of Ni(I)

compd	structure type (scheme) and electron count on metals	Ni–Ni dist, Å	ref
$[PMe_3Ni(\mu\text{-}t\text{-}Bu_2P)]_2$	A; 16,16	2.375 (3)	1
$[PMe_3Ni(\mu\text{-}(Me_3Si)_2P)]_2$	A; 16,16	2.381 (1)	6
$[C_2H_4(Ni(\mu\text{-}P(Cy)_2)_2)]_2$	A; 16,16	2.388 (1)	7
$[(Me_3P)Ni(\mu\text{-}t\text{-}Bu_2As)]_2$	A; 16,16	2.429	this work
$(PMe_3)Ni(\mu\text{-}t\text{-}Bu_2P)_2Ni(CO)_2$	B; 16,18	2.446 (2)	2
$(CO)Ni(\mu\text{-}t\text{-}Bu_2P)_2Ni(CO)_2$	B; 16,18	2.414 (2)	2
$[(CO)_2Ni(\mu\text{-}Ph_2P)]_2$	C; 18,18	2.51	8
$[(PMe_3)_2Ni(\mu\text{-}t\text{-}BuHP)]_2$	C; 18,18	2.559 (2)	9
$[(p\text{-tol-NC})_2Ni(\mu\text{-}t\text{-}Bu_2As)]_2$	C; 18,18	2.693 (2)	this work

rected. Instruments: IR, Perkin-Elmer 1330; NMR, Varian EM-390 (^{1}H, 90 MHz), FT-80 (^{31}P, 32.384 MHz). IR spectra were taken in pressed KBr disks. NMR spectra were recorded in toluene-d_8 at ambient temperature and are referenced to Me_4Si (δ 0.0, ^{1}H) or 85% H_3PO_4(aq) (δ 0.0, ^{31}P). *p*-tol-NC,[12] $NiCl_2(PMe_3)_2$,[13] and LiAs-*t*-Bu_2[14] were prepared as previously described.

$[Ni(\mu\text{-}t\text{-}Bu_2As)(PMe_3)]_2$ (Ni–Ni) (1). THF (100 mL) was added to $NiCl_2(PMe_3)_2$ (1.00 g, 3.55 mmol), and the resulting mixture was cooled to −78 °C before the addition of Li-*t*-Bu_2As (16 mL of a 0.53 M THF solution; 8.5 mmol, 2.4 equiv). The reaction mixture was stirred at −78 °C (1 h), during which time the color of the solution gradually became darker. The reaction mixture was then allowed to warm to room temperature and was stirred a further 10 h. Volatile materials were removed under vacuum, and the residue was dissolved in hexane (50 mL). This solution was filtered, concentrated (20 mL), and cooled (−5 °C) to give 0.33 g of black crystals, which were decanted from the supernatant and dried under vacuum. A further 0.10 g was obtained from the mother liquor following further evaporation and cooling: yield 0.43 g, 37%; in the determination of melting point, crystals of **1** shatter and decompose over the range 189–194 °C. ^{1}H NMR (in toluene-d_8): δ 1.43 s, ^{31}P{^{1}H} (toluene-d_8): δ 20.48 s. IR (KBr disk): 2900 vs, br, 1460 w, sh, 1448 m, 1427 w, 1411 m, 1371 w, 1349 m, 1287 w, 1268 m, 1150 s, 1006 m, 922 s, 833 w, 795 w, 705 m, 655 m, 403 w, 364 m cm^{-1}.

$[Ni(\mu\text{-}t\text{-}Bu_2As)(CN\text{-}p\text{-}tol)_2]$ (Ni–Ni) (2). Compound **1** (0.20 g, 0.31 mmol) was dissolved in hexane (35 mL) and the solution cooled to −78 °C. *p*-Tolyl isocyanide (0.22 mL, 0.21 g, 1.8 mmol, 6 equiv) was added, resulting in the immediate formation of a black microcrystalline precipitate. The solution was kept at −78 °C for 20 min and than allowed to warm to room temperature. It was then stirred for a further 12 h. Volatile materials were removed under vacuum and the red-black residue recrystallized from diethyl ether (20 mL) to give black crystals of **2**, which were collected and dried under vacuum: yield 0.14 g, 47%; mp 193–197 °C dec. IR (KBr disk): 2840 m, 2045 sh, 2000 vs, br, 1943 sh, 1605 w, 1503 m, 1380 w, 1357 w, 1260 w, 1212 w, 1160 w, 1090 w, br, 1015 w, 810 m, 727 w cm^{-1}. ^{1}H NMR (PhMe-d_8): δ 1.85 s (9 H, t-*Bu*), 1.90 s (3 H, $-C_6H_4CH_3$), 6.61–6.70 m (4 H, $-C_6H_4CH_3$).

X-ray Experimental Data

Crystals of **1** (black) and **2** (black) were mounted in thin-walled glass capillaries under nitrogen. Data were collected by the $\omega/2\theta$ scan technique at 23 ± 2 °C on an Enraf-Nonius CAD-4 diffractometer (graphite monochromator). Final lattice parameters were determined from 25 strong reflections ($26.0 > 2\theta > 30.0$). Details of data collection procedures were similar to those described in ref 15. Details of data collection parameters, crystal data, and refinements for **1** and **2** are given in Table I. For **1** systematic absences indicated a choice of *I*2/*a* or *Ia* space groups; *I*2/*a* was chosen as the correct space group on the basis of successful refinement. Data for **1** were corrected for absorption by an empirical ψ-scan method using the SDP program EAC and also for Lorentz and polarization effects. The range of transmission factors was as follows: minimum, 69.26%; maximum, 99.49%; average 90.30%. Data were collected in the $+h$, $+k$, $\pm l$ quadrants, and reflections where $h + k + l$ is odd were not collected. An agreement factor for equivalent reflections was 0.017 (intensity) and 0.013 (F_o). The coordinates of the Ni atoms were obtained from a Patternson map, and subsequent difference Fourier maps followed by least-squares refinements were used to locate the remaining atoms. A non-Poisson-contribution weighting scheme was employed for least-squares refinement with an experimental instability factor of $p = 0.03$. The function minimized in the least-squares refinement was $\sum w(|F_o| - |F_c|)^2$, where w is a weighting factor. ($w = 4(F_o)^2/\sigma_I^2 + (p(F_o)^2)^2$ for the non-Poisson contribution. σ_I is the standard deviation on I (based on counting statistics), and p is the experimental instability factor used to downweight intense reflections. No hydrogen atoms were located, and all non-hydrogen atoms were refined anisotropically. The largest peak in the final difference Fourier was 0.50 e/Å^3.

(12) Gokel, G. W.; Widera, R. P.; Weber, W. P. *Org. Synth.* **1975**, *55*, 96.
(13) Dahl, O. *Acta Chem. Scand.* **1969**, *23*, 2342.
(14) Tzschach, A.; Deylig, W. *Z. Anorg. Allg. Chem.* **1956**, *336*, 36.
(15) Jones, R. A.; Wright, T. C. *Organometallics* **1983**, *2*, 1842.

For (**2**) the space group was uniquely defined by systematic absences as $P2_1/n$. Data for **2** were corrected for absorption, Lorentz, and polarization effects as for **1**: minimum, 69.58%; maximum, 99.85%; average 93.58%. Data were collected in the $+h,+k,\pm l$ quadrant. An agreement factor for equivalent reflections was 0.024 (intensity) and 0.020 (F_o). The Ni and As positions were located by direct methods (MULTAN[16]). Subsequent difference Fourier maps followed by least-squares refinement were used to locate the remaining atoms. A non-Poisson-contribution weighting scheme was employed for least-squares refinement with an experimental instability factor of $p = 0.02$ (p is defined above).

All atoms are refined normally, but because of the limited number of observed data ($I > 3\sigma(I)$) only the nickel, arsenic, and methyl carbon atoms were refined anisotropically, and the hydrogen atoms were not located. The methyl carbon atoms in particular were chosen for anisotropic refinement because they exhibited greater thermal motion relative to the other carbon atoms, as evidenced by their larger isotropic thermal parameters. The largest peak in the final difference Fourier was 0.53e Å^{-3}.

All calculations were performed on a PDP 11/44 computer using the Enraf-Nonus software package SDP-PLUS (B. A. Frenz and Associates, College Station, TX 77840). Scattering factors were taken from ref 17. Thermal parameters and tables of observed and calculated structure factors are available.[18]

Acknowledgment. We thank the Robert A. Welch Foundation (Grant No. F-816) and the National Science Foundation (Grant No. CHE82-11883) for support. The X-ray diffractometer was purchased with funds from the NSF (Grant No. CHE82-058712) and the University of Texas.

Registry No. **1**, 100228-85-1; **2**, 100228-86-2; $NiCl_2(PMe_3)_2$, 19232-05-4; Ni, 7440-02-0.

Supplementary Material Available: Tables of general temperature factors and structure factors for **1** and **2** and least-squares planes and dihedral angles between planes for **2** (43 pages). Ordering information is given on any current masthead page.

(16) Germain, G.; Main, P.; Wolfson, M. M. *Acta Crystallogr., Sect. A: Cryst. Phys., Diffr., Theor. Gen. Crystallogr.* **1971**, *A27*, 368.

(17) "International Tables for X-ray Crystallography"; Kynoch Press: Birmingham, England, 1974; Vol. 4.

(18) See paragraph at end of text regarding supplementary material.

Contribution from the Laboratoire de Chimie-Physique, Unité Associée au CNRS No. 405, ENSCS, Université Louis Pasteur, 67000 Strasbourg, France

Spectrophotometric Study of Copper(II) Chloride–Trimethyl Phosphate Solutions. Thermodynamic and Spectroscopic Properties of Copper(II) Chloro Complexes in Nonaqueous Solutions

Chisara Amuli, Max Elleb, Jean Meullemeestre, Marie-José Schwing, and François Vierling*

Received June 24, 1985

Copper(II) chloride complexes were investigated spectrophotometrically in trimethyl phosphate solutions. A large set of UV, visible, and near-IR optical density values were computed in the numerical treatment involving least-squares and Marquardt methods. Stability and individual electronic spectra were calculated for several different theoretical models. Four mononuclear chloro complexes are the best representation of the constitution of the trimethyl phosphate solutions, and their overall formation constants are respectively $\log \beta_1 = 7.3$, $\log \beta_2 = 12.4$, $\log \beta_3 = 16.8$, and $\log \beta_4 = 19.4$. Quantitative data obtained for the chlorocuprates in terms of equilibrium constants and extinction coefficients are compared to those we have calculated earlier in six aprotic dipolar solvents. The solvation properties of the copper(II) chloride compounds were generalized by considering both the stability and the electronic spectra of the individual copper(II) chloro complexes. The stabilization of the chlorocuprates in solution is an inverse function of the donor numbers of the solvents. The calculated electronic spectra in these six solvents render it possible to classify the complexes into two groups: the cationic and neutral species for which an original crystal field parameter sequence is found; the anionic species for which the spectra demonstrate less solvation than for the cations. The d–d transition bands indicate configurational changes of copper(II), which is square planar in the cationic and neutral species and flattened tetrahedral in $CuCl_4^{2-}$, characterized in these nonaqueous media.

Introduction

Copper(II) compounds are of great interest to chemists because of their important use as catalysts in organic synthesis and to theoreticians because of their particular behavior resulting from Jahn–Teller distortion. Copper(II) chloride compounds are so commonly present in synthesis and extraction reactions that the ligand ability of the chloride ion to complexation is often omitted. The determination of the stability, electronic spectra, and structure of the copper(II) chloro complexes would promote a better understanding of the behavior of these complexes, particularly in their interactions with different nonaqueous solvents.

The lack of quantitative data of nonaqueous copper(II) chloride systems has its origin in the difficulty both of handling the experimental procedure and in the interpretation of the measurements relative to a multicomponent equilibrium.

Usual electrochemical techniques are not easily practiced: either restricted copper and ligand concentration ranges would limit the complexation or uncontrolable interferences with the solvent, the supporting electrolyte, and the copper(II) or chloride ion indicating electrode are present. These difficulties have been solved in dimethyl sulfoxide[1] and in propylene carbonate[2] media where three mononuclear copper(II) chloride species were identified.

Gutmann and co-workers[3-6] have investigated the complexation of several transition metals such as Co^{2+}, Ni^{2+}, Cu^{2+}, and Cr^{3+} with the chloride ion in different nonaqueous solutions using spectrophotometric techniques. But in general the electronic spectra were interpreted only qualitatively with some estimates of the stability constants of mononuclear complexes.

Some attempts were made to compare the spectroscopic properties of the chlorocuprates in the solid state and in solution; the assignment of the CT and d–d transition bands were essentially given for the tetrachloro complex[7,8] for which either D_{4h} or D_{2d}

(1) Foll, A.; Ledemezet, M.; Courtot-Coupez, J. *J. Electroanal. Chem. Interfacial Electrochem.* **1972**, *35*, 41.
(2) Scharff, J. P. *Bull. Soc. Chim. Fr.* **1972**, *1*, 413.
(3) Gutmann, V.; Scherhaufer, A.; Ozuba, H. *Monatsh. Chem.* **1967**, *98*, 619.
(4) Baaz, M.; Gutmann, V.; Hampel, G.; Masaguer, J. Rr. *Monatsh. Chem.* **1962**, *93*, 1416; **1963**, *94*, 822.
(5) Hubacek, H.; Stancie, B.; Gutmann, V. *Monatsh. Chem.* **1963**, *94*, 1118.
(6) Gutmann, V.; Hubner, L. *Monatsh. Chem.* **1961**, *92*, 1262.
(7) Smith, D. W. *Coord. Chem. Rev.* **1976**, *21*, 93.

0020-1669/86/1325-0856$01.50/0